

Properties of Jets in Z Boson Events from 1.8 TeV $\bar{p}p$ Collisions

F. Abe,¹⁴ H. Akimoto,³² A. Akopian,²⁷ M. G. Albrow,⁷ S. R. Amendolia,²³ D. Amidei,¹⁷ J. Antos,²⁹ C. Anway-Wiese,⁴ S. Aota,³² G. Apollinari,²⁷ T. Asakawa,³² W. Ashmanskas,¹⁵ M. Atac,⁷ F. Azfar,²² P. Azzi-Bacchetta,²¹ N. Bacchetta,²¹ W. Badgett,¹⁷ S. Bagdasarov,²⁷ M. W. Bailey,¹⁹ J. Bao,³⁵ P. De Barbaro,²⁶ A. Barbaro-Galtieri,¹⁵ V. E. Barnes,²⁵ B. A. Barnett,¹³ E. Barzi,⁸ G. Bauer,¹⁶ T. Baumann,⁹ F. Bedeschi,²³ S. Behrends,³ S. Belforte,²³ G. Bellettini,²³ J. Bellinger,³⁴ D. Benjamin,³¹ J. Benloch,¹⁶ J. Bensingler,³ D. Benton,²² A. Beretvas,⁷ J. P. Berge,⁷ J. Berryhill,⁵ S. Bertolucci,⁸ A. Bhatti,²⁷ K. Biery,¹² M. Binkley,⁷ D. Bisello,²¹ R. E. Blair,¹ C. Blocker,³ A. Bodek,²⁶ W. Bokhari,¹⁶ V. Bolognesi,⁷ D. Bortoletto,²⁵ J. Boudreau,²⁴ L. Breccia,² C. Bromberg,¹⁸ N. Bruner,¹⁹ E. Buckley-Geer,⁷ H. S. Budd,²⁶ K. Burkett,¹⁷ G. Busetto,²¹ A. Byon-Wagner,⁷ K. L. Byrum,¹ J. Cammerata,¹³ C. Campagnari,⁷ M. Campbell,¹⁷ A. Caner,⁷ W. Carithers,¹⁵ D. Carlsmith,³⁴ A. Castro,²¹ D. Cauz,²³ Y. Cen,²⁶ F. Cervelli,²³ P. S. Chang,²⁹ P. T. Chang,²⁹ H. Y. Chao,²⁹ J. Chapman,¹⁷ M.-T. Cheng,²⁹ G. Chiarelli,²³ T. Chikamatsu,³² C. N. Chiou,²⁹ L. Christofek,¹¹ S. Cihangir,⁷ A. G. Clark,²³ M. Cobal,²³ M. Contreras,⁵ J. Conway,²⁸ J. Cooper,⁷ M. Cordelli,⁸ C. Couyoumtzelis,²³ D. Crane,¹ D. Cronin-Hennessy,⁶ R. Culbertson,⁵ J. D. Cunningham,³ T. Daniels,¹⁶ F. DeJongh,⁷ S. Delchamps,⁷ S. Dell'Agnello,²³ M. Dell'Orso,²³ L. Demortier,²⁷ B. Denby,²³ M. Deninno,² P. F. Derwent,¹⁷ T. Devlin,²⁸ J. R. Dittmann,⁶ S. Donati,²³ J. Done,³⁰ T. Dorigo,²¹ A. Dunn,¹⁷ N. Eddy,¹⁷ K. Einsweiler,¹⁵ J. E. Elias,⁷ R. Ely,¹⁵ E. Engels, Jr.,²⁴ D. Errede,¹¹ S. Errede,¹¹ Q. Fan,²⁶ I. Fiori,² B. Flaughner,⁷ G. W. Foster,⁷ M. Franklin,⁹ M. Frautschi,³¹ J. Freeman,⁷ J. Friedman,¹⁶ H. Frisch,⁵ T. A. Fuess,¹ Y. Fukui,¹⁴ S. Funaki,³² G. Gagliardi,²³ S. Galeotti,²³ M. Gallinaro,²¹ M. Garcia-Sciveres,¹⁵ A. F. Garfinkel,²⁵ C. Gay,⁹ S. Geer,⁷ D. W. Gerdes,¹⁷ P. Giannetti,²³ N. Giokaris,²⁷ P. Giromini,⁸ L. Gladney,²² D. Glenzinski,¹³ M. Gold,¹⁹ J. Gonzalez,²² A. Gordon,⁹ A. T. Goshaw,⁶ K. Goulianos,²⁷ H. Grassmann,²³ L. Groer,²⁸ C. Grosso-Pilcher,⁵ G. Guillian,¹⁷ R. S. Guo,²⁹ C. Haber,¹⁵ E. Hafen,¹⁶ S. R. Hahn,⁷ R. Hamilton,⁹ R. Handler,³⁴ R. M. Hans,³⁵ K. Hara,³² A. D. Hardman,²⁵ B. Harral,²² R. M. Harris,⁷ S. A. Hauger,⁶ J. Hauser,⁴ C. Hawk,²⁸ E. Hayashi,³² J. Heinrich,²² K. D. Hoffman,²⁵ M. Hohlmann,^{1,5} C. Holck,²² R. Hollebeek,²² L. Holloway,¹¹ A. Hölscher,¹² S. Hong,¹⁷ G. Houk,²² P. Hu,²⁴ B. T. Huffman,²⁴ R. Hughes,²⁶ J. Huston,¹⁸ J. Huth,⁹ J. Huyen,⁷ H. Ikeda,³² M. Incagli,²³ J. Incandela,⁷ G. Introzzi,²³ J. Iwai,³² Y. Iwata,¹⁰ H. Jensen,⁷ U. Joshi,⁷ R. W. Kadel,¹⁵ E. Kajfasz,^{7,*} T. Kamon,³⁰ T. Kaneko,³² K. Karr,³³ H. Kasha,³⁵ Y. Kato,²⁰ T. A. Keaffaber,²⁵ L. Keeble,⁸ K. Kelley,¹⁶ R. D. Kennedy,²⁸ R. Kephart,⁷ P. Kesten,¹⁵ D. Kestenbaum,⁹ R. M. Keup,¹¹ H. Keutelian,⁷ F. Keyvan,⁴ B. Kharadia,¹¹ B. J. Kim,²⁶ D. H. Kim,⁷ H. S. Kim,¹² S. B. Kim,¹⁷ S. H. Kim,³² Y. K. Kim,¹⁵ L. Kirsch,³ P. Koehn,²⁶ K. Kondo,³² J. Konigsberg,⁹ S. Kopp,⁵ K. Kordas,¹² W. Koska,⁷ E. Kovacs,⁷ W. Kowald,⁶ M. Krasberg,¹⁷ J. Kroll,⁷ M. Kruse,²⁵ T. Kuwabara,³² S. E. Kuhlmann,¹ E. Kuns,²⁸ A. T. Laasanen,²⁵ N. Labanca,²³ S. Lammel,⁷ J. I. Lamoureux,³ T. LeCompte,¹¹ S. Leone,²³ J. D. Lewis,⁷ P. Limon,⁷ M. Lindgren,⁴ T. M. Liss,¹¹ N. Lockyer,²² O. Long,²² C. Loomis,²⁸ M. Loretto,²¹ J. Lu,³⁰ D. Lucchesi,²³ P. Lukens,⁷ S. Lusin,³⁴ J. Lys,¹⁵ K. Maeshima,⁷ A. Maghakian,²⁷ P. Maksimovic,¹⁶ M. Mangano,²³ J. Mansour,¹⁸ M. Mariotti,²¹ J. P. Marriner,⁷ A. Martin,¹¹ J. A. J. Matthews,¹⁹ R. Mattingly,¹⁶ P. McIntyre,³⁰ P. Melese,²⁷ A. Menzione,²³ E. Meschi,²³ S. Metzler,²² C. Miao,¹⁷ G. Michail,⁹ R. Miller,¹⁸ H. Minato,³² S. Miscetti,⁸ M. Mishina,¹⁴ H. Mitsushio,³² T. Miyamoto,³² S. Miyashita,³² Y. Morita,¹⁴ J. Mueller,²⁴ A. Mukherjee,⁷ T. Muller,⁴ P. Murat,²³ H. Nakada,³² I. Nakano,³² C. Nelson,⁷ D. Neuberger,⁴ C. Newman-Holmes,⁷ M. Ninomiya,³² L. Nodulman,¹ S. H. Oh,⁶ K. E. Ohl,³⁵ T. Ohmoto,¹⁰ T. Ohsugi,¹⁰ R. Oishi,³² M. Okabe,³² T. Okusawa,²⁰ R. Oliver,²² J. Olsen,³⁴ C. Pagliarone,² R. Paoletti,²³ V. Papadimitriou,³¹ S. P. Pappas,³⁵ S. Park,⁷ A. Parri,⁸ J. Patrick,⁷ G. Pauletta,²³ M. Paulini,¹⁵ A. Perazzo,²³ L. Pescara,²¹ M. D. Peters,¹⁵ T. J. Phillips,⁶ G. Piacentino,² M. Pillai,²⁶ K. T. Pitts,⁷ R. Plunkett,⁷ L. Pondrom,³⁴ J. Proudfoot,¹ F. Ptohos,⁹ G. Punzi,²³ K. Ragan,¹² A. Ribon,²¹ F. Rimondi,² L. Ristori,²³ W. J. Robertson,⁶ T. Rodrigo,⁷ S. Rolli,²³ J. Romano,⁵ L. Rosenson,¹⁶ R. Roser,¹¹ W. K. Sakumoto,²⁶ D. Saltzberg,⁵ A. Sansoni,⁸ L. Santi,²³ H. Sato,³² V. Scarpine,³⁰ P. Schlabach,⁹ E. E. Schmidt,⁷ M. P. Schmidt,³⁵ A. Scribano,²³ S. Segler,⁷ S. Seidel,¹⁹ Y. Seiya,³² G. Sganos,¹² A. Sgolacchia,² M. D. Shapiro,¹⁵ N. M. Shaw,²⁵ Q. Shen,²⁵ P. F. Shepard,²⁴ M. Shimojima,³² M. Shochet,⁵ J. Siegrist,¹⁵ A. Sill,³¹ P. Sinervo,¹² P. Singh,²⁴ J. Skarha,¹³ K. Sliwa,³³ F. D. Snider,¹³ T. Song,¹⁷ J. Spalding,⁷ P. Sphicas,¹⁶ F. Spinella,²³ M. Spiropulu,⁹ L. Spiegel,⁷ L. Stanco,²¹ J. Steele,³⁴ A. Stefanini,²³ K. Strahl,¹² J. Strait,⁷ R. Ströhmer,⁹ D. Stuart,⁷ G. Sullivan,⁵ A. Soumarokov,²⁹ K. Sumorok,¹⁶ J. Suzuki,³² T. Takada,³² T. Takahashi,²⁰ T. Takano,³² K. Takikawa,³² N. Tamura,¹⁰ F. Tartarelli,²³ W. Taylor,¹² P. K. Teng,²⁹ Y. Teramoto,²⁰ S. Tether,¹⁶ D. Theriot,⁷ T. L. Thomas,¹⁹ R. Thun,¹⁷ M. Timko,³³ P. Tipton,²⁶ A. Titov,²⁷ S. Tkaczyk,⁷ D. Toback,⁵ K. Tollefson,²⁶ A. Tollestrup,⁷

J. Tonnison,²⁵ J. F. De Troconiz,⁹ S. Truitt,¹⁷ J. Tseng,¹³ N. Turini,²³ T. Uchida,³² N. Uemura,³² F. Ukegawa,²² G. Unal,²² S. C. Van Den Brink,²⁴ S. Vejcik III,¹⁷ G. Velev,²³ R. Vidal,⁷ M. Vondracek,¹¹ D. Vucinic,¹⁶ R. G. Wagner,¹ R. L. Wagner,⁷ J. Wahl,⁵ C. Wang,⁶ C. H. Wang,²⁹ G. Wang,²³ J. Wang,⁵ M. J. Wang,²⁹ Q. F. Wang,²⁷ A. Warburton,¹² T. Watts,²⁸ R. Webb,³⁰ C. Wei,⁶ C. Wendt,³⁴ H. Wenzel,¹⁵ W. C. Wester III,⁷ A. B. Wicklund,¹ E. Wicklund,⁷ R. Wilkinson,²² H. H. Williams,²² P. Wilson,⁵ B. L. Winer,²⁶ D. Wolinski,¹⁷ J. Wolinski,¹⁸ X. Wu,²³ J. Wyss,²¹ A. Yagil,⁷ W. Yao,¹⁵ K. Yasuoka,³² Y. Ye,¹² G. P. Yeh,⁷ P. Yeh,²⁹ M. Yin,⁶ J. Yoh,⁷ C. Yosef,¹⁸ T. Yoshida,²⁰ D. Yovanovitch,⁷ I. Yu,³⁵ L. Yu,¹⁹ J. C. Yun,⁷ A. Zanetti,²³ F. Zetti,²³ L. Zhang,³⁴ W. Zhang,²² B. Zou,⁶ and S. Zucchelli²

(CDF Collaboration)

¹Argonne National Laboratory, Argonne, Illinois 60439

²Istituto Nazionale di Fisica Nucleare, University of Bologna, I-40126 Bologna, Italy

³Brandeis University, Waltham, Massachusetts 02254

⁴University of California at Los Angeles, Los Angeles, California 90024

⁵University of Chicago, Chicago, Illinois 60637

⁶Duke University, Durham, North Carolina 27708

⁷Fermi National Accelerator Laboratory, Batavia, Illinois 60510

⁸Laboratori Nazionali di Frascati, Istituto Nazionale di Fisica Nucleare, I-00044 Frascati, Italy

⁹Harvard University, Cambridge, Massachusetts 02138

¹⁰Hiroshima University, Higashi-Hiroshima 724, Japan

¹¹University of Illinois, Urbana, Illinois 61801

¹²Institute of Particle Physics, McGill University, Montreal, Canada H3A 2T8
and University of Toronto, Toronto, Canada M5S 1A7

¹³The Johns Hopkins University, Baltimore, Maryland 21218

¹⁴National Laboratory for High Energy Physics (KEK), Tsukuba, Ibaraki 305, Japan

¹⁵Lawrence Berkeley Laboratory, Berkeley, California 94720

¹⁶Massachusetts Institute of Technology, Cambridge, Massachusetts 02139

¹⁷University of Michigan, Ann Arbor, Michigan 48109

¹⁸Michigan State University, East Lansing, Michigan 48824

¹⁹University of New Mexico, Albuquerque, New Mexico 87131

²⁰Osaka City University, Osaka 588, Japan

²¹Universita di Padova, Istituto Nazionale di Fisica Nucleare, Sezione di Padova, I-35131 Padova, Italy

²²University of Pennsylvania, Philadelphia, Pennsylvania 19104

²³Istituto Nazionale di Fisica Nucleare, University and Scuola Normale Superiore of Pisa, I-56100 Pisa, Italy

²⁴University of Pittsburgh, Pittsburgh, Pennsylvania 15260

²⁵Purdue University, West Lafayette, Indiana 47907

²⁶University of Rochester, Rochester, New York 14627

²⁷Rockefeller University, New York, New York 10021

²⁸Rutgers University, Piscataway, New Jersey 08854

²⁹Academia Sinica, Taipei, Taiwan 11529, Republic of China

³⁰Texas A&M University, College Station, Texas 77843

³¹Texas Tech University, Lubbock, Texas 79409

³²University of Tsukuba, Tsukuba, Ibaraki 305, Japan

³³Tufts University, Medford, Massachusetts 02155

³⁴University of Wisconsin, Madison, Wisconsin 53706

³⁵Yale University, New Haven, Connecticut 06511

(Received 7 March 1996)

We present a study of events with Z bosons and hadronic jets produced in $\bar{p}p$ collisions at a center-of-mass energy of 1.8 TeV. The data consist of 6708 $Z \rightarrow e^+e^-$ decays from 106 pb^{-1} of integrated luminosity collected using the CDF detector at the Fermilab Tevatron Collider. The $Z + \geq n$ jet cross sections and jet production properties have been measured for $n = 1$ to 4. The data are compared to predictions of leading-order QCD matrix element calculations with added gluon radiation and simulated parton fragmentation. [S0031-9007(96)00694-1]

PACS numbers: 13.87.Ce, 12.38.Qk, 13.85.Qk

Since the 1983 discovery of the Z boson at CERN [1,2], the hadronic production properties of the Z have been studied using relatively small event samples, most recently from experiments at the Fermilab Tevatron Collider

[3]. In this Letter we describe an extension of these studies based on a much larger sample of 6708 $Z \rightarrow e^+e^-$ decays obtained from 106 pb^{-1} of integrated $\bar{p}p$ luminosity using the CDF detector. This event sample is large

enough to study the production properties of high energy hadronic jets associated with Z boson production, and provides a good test of quantum chromodynamics (QCD) calculations since the backgrounds are small and the presence of the Z selects high Q^2 parton-level processes. A determination of the reliability of QCD calculations for heavy boson production is important for verifying the direct W boson backgrounds to top quark production [4,5]. Z boson events are free of top quark contamination and provide a clean test of standard model heavy boson production. As part of this study we examine the Z boson sample for evidence of excess b quark decays that could indicate new particle production.

The elements of the CDF detector of primary importance to this analysis are the central tracking chamber (CTC), the calorimeters, and the silicon vertex detector (SVX). The CTC, which is immersed in a 1.4 T solenoidal magnetic field, measures the momenta and trajectories of charged particles in the region $|\eta| < 1.1$ [6]. The calorimeters are divided into electromagnetic and hadronic components and cover the pseudorapidity range $|\eta| < 4.2$. The four-layer SVX [7], located just outside the beam pipe, provides precise tracking in the plane transverse to the beam direction and is used to reconstruct secondary vertices from b decays. The CDF detector is described in detail elsewhere [4,8].

We identify $Z \rightarrow e^+e^-$ candidates in events passing a high transverse energy (E_T) electron trigger. The event selection requires an isolated electron [9] with $E_T \geq 20$ GeV in the central calorimeter ($|\eta| \leq 1.1$) that satisfies tight selection cuts [10] and has a CTC track. A second electron, satisfying looser selection cuts, is required in the central, plug ($1.1 \leq |\eta| \leq 2.4$), or forward ($2.4 \leq |\eta| \leq 3.7$) calorimeter with $E_T \geq 20, 15,$ or 10 GeV, respectively. We remove electrons with photon conversion characteristics. The separation in η - ϕ between the centroid of an electron calorimeter cluster and that of any jet in the event, measured in $\Delta R = \sqrt{\Delta\eta^2 + \Delta\phi^2}$, must exceed $\Delta R = 0.52$.

We select an event sample of 6708 $Z \rightarrow e^+e^-$ decays by requiring the electron pair masses to lie within $15 \text{ GeV}/c^2$ of the nominal Z boson mass of $91 \text{ GeV}/c^2$. The background in these data and the $Z \rightarrow e^+e^-$ acceptance due to our selection cuts are measured as a function of associated jet multiplicity as described below.

Hadronic jets produced in association with the Z bosons are selected using a clustering algorithm [11] with a cone size of $R_j = 0.4$. The jet energies are corrected to account for variations in calorimeter response, fragmentation energy outside the jet cone, and underlying event energy within the jet cone. When the separation between two jets with $E_T \geq 12$ GeV is less than $\Delta R = 0.52$, they are combined vectorially into a single jet. Jets with $E_T \geq 15$ GeV and $|\eta| \leq 2.4$ are selected for this analysis. Of the 6708 Z events, 1310 have ≥ 1 jet, 279 have ≥ 2 jets, 57 have ≥ 3 jets, and 11 have ≥ 4 jets. We correct these jet multiplici-

ties for two additional effects: photons counted as hadronic jets, and jets produced in extra $\bar{p}p$ interactions that occur in the same bunch crossing as the Z event. A Z + photon Monte Carlo calculation [12] with detector simulation yields a correction varying from -2% to -3% for photons as a function of jet multiplicity. Using minimum bias events, we estimate the number of jets from additional interactions that pass the selection cuts, and obtain corrections varying from -3% to -5% .

The backgrounds to the Z boson are dominated by jets faking electrons, but include some contributions from heavy quark, $W \rightarrow e\nu + \text{jet}$, and $Z \rightarrow \tau^+\tau^-$ decays. To measure the background we employ a data sample in which all Z boson selection cuts have been applied, except the mass window and electron isolation cuts. By selecting events from this sample in which neither electron candidate is isolated, we obtain a set of events that is almost entirely background with no measurable contribution from $Z \rightarrow e^+e^-$. The mass distribution for these background events is independent of electron candidate isolation. This allows us to estimate the number of background events with isolated electrons that lie within the mass window. We obtain background estimates in the Z boson event sample that are small even at high jet multiplicities, with 1σ upper limits of 1.1%, 2.3%, 3.0%, and 4.0% for the $n \geq 0, 1, 2,$ and 3 jet events, respectively.

The acceptance for electrons from Z boson decays has been measured as a function of the number of associated hadronic jets. Losses due to the electron E_T cuts and detector geometric acceptance have been studied using an inclusive Z boson production model and a leading-order Z + jets QCD calculation [13]. The loss of electrons due to overlap with jets and the efficiency of the electron-jet separation cut are determined by selecting $Z \rightarrow e^+e^-$ data events with jets and using a Monte Carlo program to redecay the Z bosons. A final acceptance correction is made for electron identification cuts and the efficiency of the online trigger, which selects high- E_T central electrons. The total $Z \rightarrow e^+e^-$ detection efficiencies vary from $(37.3 \pm 0.7)\%$ for Z bosons without jets to $(31.5 \pm 1.4)\%$ for Z bosons with ≥ 4 jets.

The systematic uncertainties on the number of jets due to the jet selection cuts are determined by varying the jet energy scale by $\pm 5\%$, the $|\eta|$ cut by ± 0.2 , the underlying event correction by $\pm 50\%$, the photon removal correction by $\pm 15\%$, and the probability of jets from additional $\bar{p}p$ interactions by $\pm 100\%$. The total jet-counting uncertainties are found to range between 11% for the ≥ 1 jet to 23% for the ≥ 4 jet sample and dominate the uncertainties in the cross section measurements, except for $Z \rightarrow \geq 4$ jet events where the statistical error is larger.

We measure the cross section for Z production as a function of jet multiplicity using the ratio of the number of detected Z events with $\geq n$ jets to the total number of detected Z events. The cross sections are determined from these ratios using the inclusive Z boson cross section of 231 ± 12 pb [14] and the ratios of

TABLE I. $Z + \geq n$ jet cross sections. The first error on the data cross sections is the statistical error; the second includes the systematic error on the Z acceptance and the luminosity error added in quadrature. For $n = 1$ to 4, the second error also includes the jet-counting uncertainty, as described in the text. The leading-order (LO) Monte Carlo cross sections are generated with VECBOS for Q^2 scales of $\langle p_T \rangle^2$ and $M_Z^2 + p_{Tz}^2$. The ≥ 0 jet calculation is next-to-next-to-leading order (NNLO) with $Q^2 = M_Z^2$. The error on the NNLO QCD cross section includes systematic and statistical uncertainties; for the LO cross sections the errors are statistical.

| n Jets | $B\sigma_{\text{Data}}$ | $Q^2 = \langle p_T \rangle^2$ | | $Q^2 = M_Z^2 + p_{Tz}^2$ | | $\sigma(n)/\sigma(n-1)$ (Data) |
|-------------|--------------------------|-------------------------------|--|-----------------------------|--|-----------------------------------|
| | (pb) | $B\sigma_{\text{QCD}}$ (pd) | $\sigma_{\text{Data}}/\sigma_{\text{QCD}}$ | $B\sigma_{\text{QCD}}$ (pb) | $\sigma_{\text{Data}}/\sigma_{\text{QCD}}$ | |
| ≥ 0 | $231 \pm 6 \pm 11$ | ... | ... | 223 ± 10 | 1.04 ± 0.07 | ... |
| ≥ 1 | $45.2 \pm 1.2 \pm 5.7$ | 35.16 ± 0.54 | 1.29 ± 0.17 | 26.82 ± 0.40 | 1.69 ± 0.22 | 0.196 ± 0.007 |
| ≥ 2 | $9.7 \pm 0.6 \pm 1.8$ | 10.53 ± 0.38 | 0.92 ± 0.19 | 5.77 ± 0.16 | 1.68 ± 0.34 | 0.215 ± 0.014 |
| ≥ 3 | $2.03 \pm 0.28 \pm 0.49$ | 2.44 ± 0.17 | 0.83 ± 0.24 | 1.23 ± 0.08 | 1.66 ± 0.47 | 0.210 ± 0.027 |
| ≥ 4 | $0.43 \pm 0.13 \pm 0.11$ | | | | | 0.211 ± 0.059 |

detection efficiencies. This method takes advantage of the cancellation of some systematic uncertainties in the ratios, and gives the most accurate relative $Z + \geq n$ jet cross sections. The measured cross sections for $Z + \geq n$ ($n = 1$ to 4) jet events are given in Table I, as are the measured ratios of $\sigma(Z + \geq n \text{ jets})/\sigma(Z + \geq n - 1 \text{ jets})$, which are constant at ~ 0.2 for $n = 1$ to 4.

The measured cross sections and the production characteristics of the hadronic jets can be compared to QCD calculations. The leading-order matrix element calculations for $Z + n$ parton events (for $n = 1, 2, 3$) are obtained with the VECBOS [13] Monte Carlo program [15]. We use both MRSA and CTEQ3M parton distribution functions, the two-loop α_s evolution, and factorization and renormalization scales varying from $Q^2 = M_Z^2 + p_{Tz}^2$ of the Z boson to $Q^2 = \langle p_T \rangle^2$, where $\langle p_T \rangle$ is the average p_T of the generated partons. The QCD predictions are indistinguishable for the two parton distribution functions within the statistical uncertainties of our calculation.

The QCD-predicted $Z +$ jet events are obtained from the parton-level events by including gluon radiation and hadronic fragmentation using the HERWIG [16] shower simulation algorithm [17]. This procedure represents a

partial higher-order correction to tree-level diagrams. The Z boson events with hadron showers are then introduced into a full CDF detector simulation, and the resulting jets are identified and selected as in the data. This allows us to make direct comparisons between the QCD predictions and data.

The Monte Carlo events passing our jet selection cuts are used to determine QCD-predicted cross sections that are compared to the experimental measurements corrected for $Z \rightarrow e^+e^-$ decay losses and backgrounds. The calculated QCD cross sections are given in Table I, and compared to the data via ratios of the measured to QCD-predicted cross sections. Figure 1 shows a plot of the measured cross sections for $Z + \geq n$ jets as a function of n , with the QCD predictions resulting from variations in Q^2 indicated by a superimposed band. For $Q^2 = \langle p_T \rangle^2$, the measured $Z + \geq n$ jet cross sections range from 0.83 to 1.29 times the leading-order QCD predictions. For $Q^2 = M_Z^2 + p_{Tz}^2$, the ratios of cross sections to leading-

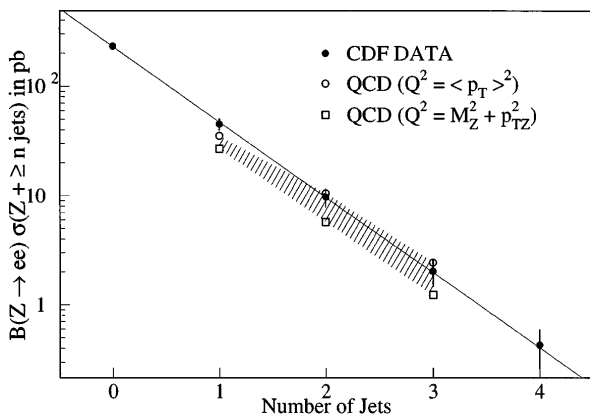


FIG. 1. Cross section for $Z + \geq n$ jets versus n , for $Z \rightarrow e^+e^-$. The QCD-prediction band spans two different renormalization scales. The line is an exponential fit to the measured cross sections. The error bars include statistical and systematic uncertainties.

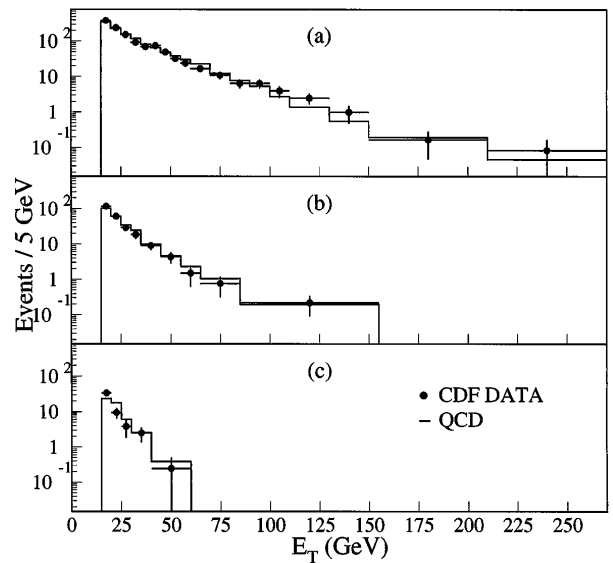


FIG. 2. Transverse energy of the (a) first, (b) second, and (c) third highest E_T jets in ≥ 1 , ≥ 2 , and ≥ 3 jet events, respectively. The points are data (statistical errors only), and the histograms are the QCD predictions normalized to the data.

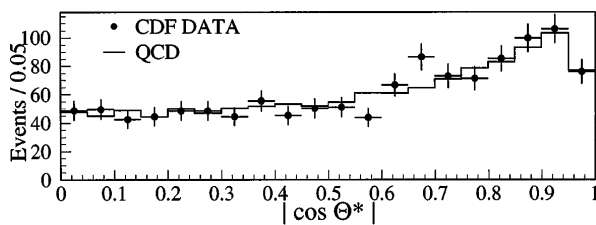


FIG. 3. The $|\cos \Theta^*|$ distribution (see text) of the Z in ≥ 1 jet events. The acceptance decreases substantially as $|\cos \Theta^*|$ approaches 1. The Monte Carlo predictions are normalized to the data, and the data errors are statistical only.

order QCD predictions for each n are larger, but nearly constant at 1.7.

To compare the jet production properties of Z + jets events with QCD predictions, we use the same Monte Carlo event generation described above but apply both $Z \rightarrow e^+e^-$ and jet selection cuts. The QCD-predicted event distributions with $Q^2 = \langle p_T \rangle^2$ are normalized to the number of events in the data samples. Corrections are made for photons counted as jets and for jets from extra $\bar{p}p$ interactions, but no corrections are made for the small Z boson backgrounds. Figure 2 shows the E_T spectra for the (a) first, (b) second, and (c) third jets (ordered by decreasing E_T) in the ≥ 1 , ≥ 2 , and ≥ 3 jet Z events, respectively. The values of the χ^2 per degree of freedom are (a) 25/15, (b) 4.8/6, and (c) 8.3/3, using only statistical errors. In the $Z + \geq 1$ jet event sample we measure the angle Θ^* between the Z boson and the average beam direction in the Z + leading jet center-of-mass frame. The distribution of the quantity $|\cos \Theta^*|$, shown in Fig. 3, agrees well with the QCD predictions ($\chi^2 = 16.9/19$). In events with two or more jets, we measure the separation in η - ϕ space between the two leading jets. The resulting ΔR_{jj} distribution (with no photon correction) is given in Fig. 4 ($\chi^2 = 8.0/7$). The QCD-predicted ΔR_{jj} distribution is sensitive to the manner in which gluon radiation is added to the VECBOS matrix element by the HERWIG algorithm [17].

We use a secondary vertex algorithm employed by CDF for the top quark search [4,5] to examine the Z + jets data for evidence of b quark decays measured by the SVX. Of the 1665 jets in the sample, 442 are candidates for secondary vertex reconstruction, meaning that they have at least two tracks in the SVX, an uncorrected jet $E_T >$

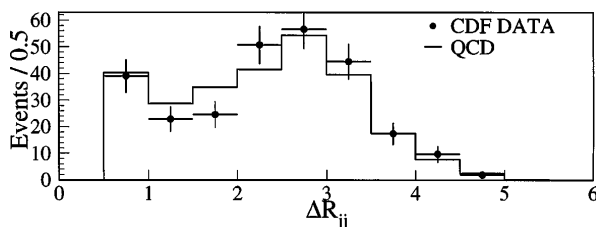


FIG. 4. Separation in η - ϕ space between the two leading jets in $Z + \geq 2$ jet events. The Monte Carlo predictions are normalized to the data. The data errors are statistical only.

15 GeV, and $|\eta| < 2$. A control sample of inclusive jet events is used to determine the number of secondary vertices expected from jets in QCD events with no heavy boson. In all, six secondary vertex candidates are found in the data sample where 6.3 ± 1.0 are expected.

In summary, this Letter contains an analysis of jet production properties associated with $Z \rightarrow e^+e^-$ events selected from 106 pb^{-1} of $\bar{p}p$ collisions at a center-of-mass energy of 1.8 TeV. We compare the data to leading-order matrix elements with HERWIG-simulated parton showers and fragmentation. The ratios of the measured cross sections to those predicted by QCD vary from 1.29 ± 0.17 to 1.69 ± 0.22 for $\bar{p}p \rightarrow Z + \geq 1$ jet when the Q^2 scale is varied from $\langle p_T \rangle^2$ to $M_Z^2 + p_{Tz}^2$. The QCD-predicted jet production properties are in generally good agreement with the measured distributions. The incidence of b quark decays in the jets associated with Z bosons is consistent with that observed in similar jets from events with no heavy boson.

We thank the Fermilab staff and the technical staffs of the participating institutions for their vital contributions. We also thank Walter Giele, Vernon Barger, Nigel Glover, and Tim Stelzer for many useful discussions. This work was supported by the U.S. Department of Energy and National Science Foundation; the Italian Istituto Nazionale di Fisica Nucleare; the Ministry of Education, Science and Culture of Japan; the Natural Sciences and Engineering Research Council of Canada; the National Science Council of the Republic of China; and the A. P. Sloan Foundation.

*Visitor.

- [1] G. Arnison *et al.*, Phys. Lett. **126B**, 398 (1983).
- [2] P. Bagnaia *et al.*, Phys. Lett. **129B**, 130 (1983).
- [3] F. Abe *et al.*, Phys. Rev. Lett. **67**, 2937 (1991).
- [4] F. Abe *et al.*, Phys. Rev. D **50**, 2966 (1994).
- [5] F. Abe *et al.*, Phys. Rev. Lett. **74**, 2626 (1995).
- [6] We use a polar coordinate system in which z is along the proton direction, ϕ is the azimuthal angle, and θ is the polar angle. Pseudorapidity, $\eta = -\ln[\tan(\theta/2)]$, is calculated using $z = 0$ at the center of the detector for fiducial cuts and at the interaction point for ΔR cones.
- [7] D. Amidei *et al.*, Nucl. Instrum. Methods Phys. Res., Sect. A **350**, 73 (1994).
- [8] F. Abe *et al.*, Nucl. Instrum. Methods Phys. Res., Sect. A **271**, 387 (1988).
- [9] An isolated electron is one for which the transverse calorimeter energy in a cone of radius 0.4 in η - ϕ around the electron cluster is less than 10% of the electron E_T .
- [10] F. Abe *et al.*, Phys. Rev. D **44**, 29 (1991). Our selection cuts are the same as those in this reference except for (i) $0.5 < E/p < 2.0$ and (ii) $\chi_{\text{strip}}^2 < 10$.
- [11] F. Abe *et al.*, Phys. Rev. D **45**, 1448 (1992).
- [12] U. Baur and E. L. Berger, Phys. Rev. D **47**, 4889 (1993).
- [13] F. A. Berends, W. T. Giele, H. Kuijff, and B. Tausk, Nucl. Phys. **B357**, 32 (1991).
- [14] F. Abe *et al.*, Phys. Rev. Lett. **76**, 3070 (1996).

-
- [15] We generate $Z +$ parton events with parton $p_T > 8 \text{ GeV}/c$, $|\eta| < 3.5$, and $\Delta R > 0.4$ between partons.
- [16] G. Marchesini and B. Webber, Nucl. Phys. **B310**, 461 (1988); G. Marchesini *et al.*, Comput. Phys. Commun. **67**, 465 (1992).
- [17] The HERWIG initial state radiation contributes jets to the Z boson event. For our calculation, a kinematic limit of $\sqrt{M_Z^2 + p_{Tz}^2}$ is applied to the gluon radiation.